Publ. Astron. Soc. Japan 38, 475–483 (1986)

43-GHz Continuum Observations of the Galactic Center

Yoshiaki SOFUE,* Makoto INOUE, Toshihiro HANDA, Masato TSUBOI, Hisashi HIRABAYASHI, Masaki MORIMOTO, and Kenji AKABANE

Nobeyama Radio Observatory,† Minamimaki-mura, Minamisaku-gun, Nagano 384-13

(Received 1985 December 13; accepted 1986 April 2)

Abstract

The galactic center region including Sgr A, the radio "bridge" and "arc" was mapped in the radio continuum at 43 GHz using the 45-m telescope with a HPBW of 38″. The Sgr A halo is resolved into some spurs and ridges, and the bridge into two complex filaments. The arc is also resolved into two straight filaments. The spectral indices for discrete sources were obtained between 43 and 10 GHz. Most of the sources have flat spectra. The radio arc, which appears to be nonthermal, has also a flat spectrum. This may indicate that high-energy electrons are being supplied or accelerated in the arc in a time scale of a few times 10^6 yr.

Key words: Galactic center; Nucleus activity; Radio continuum emission; Sgr A.

1. Introduction

Radio continuum mapping of the central region of the Galaxy has been made at various frequencies from metric to centimetric wavelengths [80 MHz: LaRosa and Kassim (1985); 160 MHz: Dulk and Slee (1974); 408 MHz: Little (1974); 610 MHz: Downes et al. (1978); 843 MHz: Mills and Drinkwater (1984); 1.6 GHz: Yusef-Zadeh et al. (1984); 2.7 GHz: Reich et al. (1984); 5 GHz: Altenhoff et al. (1979), 10.7 GHz: Pauls et al. 1976; 15.5 GHz: Kapitzky and Dent (1974); see also Oort (1977, 1985) and Brown and Liszt (1984)]. Among them recent VLA observations at 20 cm (Yusef-Zadeh et al. 1984) revealed thin filamentary structures along the radio arc. The arc is connected to the more complicated filamentary bridge running toward Sgr A, and Sgr A is surrounded by a fuzzy halo. Also the recent detection of a high-degree linear polarization and an extremely large rotation measure along the radio arc (Inoue et al. 1984; Tsuboi et al. 1985; Seiradakis et al. 1985; Yusef-Zadeh et al. 1985) called further attention to the nonthermal nature related to a magnetic field despite the flat radio spectrum so far known up to 10 GHz (Sofue and Handa 1984; Sofue 1985).

* Present address: Department of Astronomy, Faculty of Science, University of Tokyo, Bunkyo-ku, Tokyo 113.

† Nobeyama Radio Observatory, a branch of the Tokyo Astronomical Observatory, University of Tokyo, is a facility open for general use by researchers in the field of astronomy and astrophysics.

Although there is much information about the morphology of these peculiar features at low frequencies, we lack high-resolution imaging in the millimetric wave range. To get such an image and information like the spectral-index variation at higher frequencies, we performed a radio-continuum mapping at 43.25 GHz of the central region surrounding Sgr A and the radio arc. This is the highest-frequency mapping of this region so far done.

2. Observations

The observations were made in May and June, 1985 as part of the radio-continuum survey of the galactic plane in the millimeter-wave range at NRO, and were successfully done on two clear nights. We used the 45-m telescope which was equipped with a Schottky-barrier diode-mixer receiver combined with a parametric amplifier

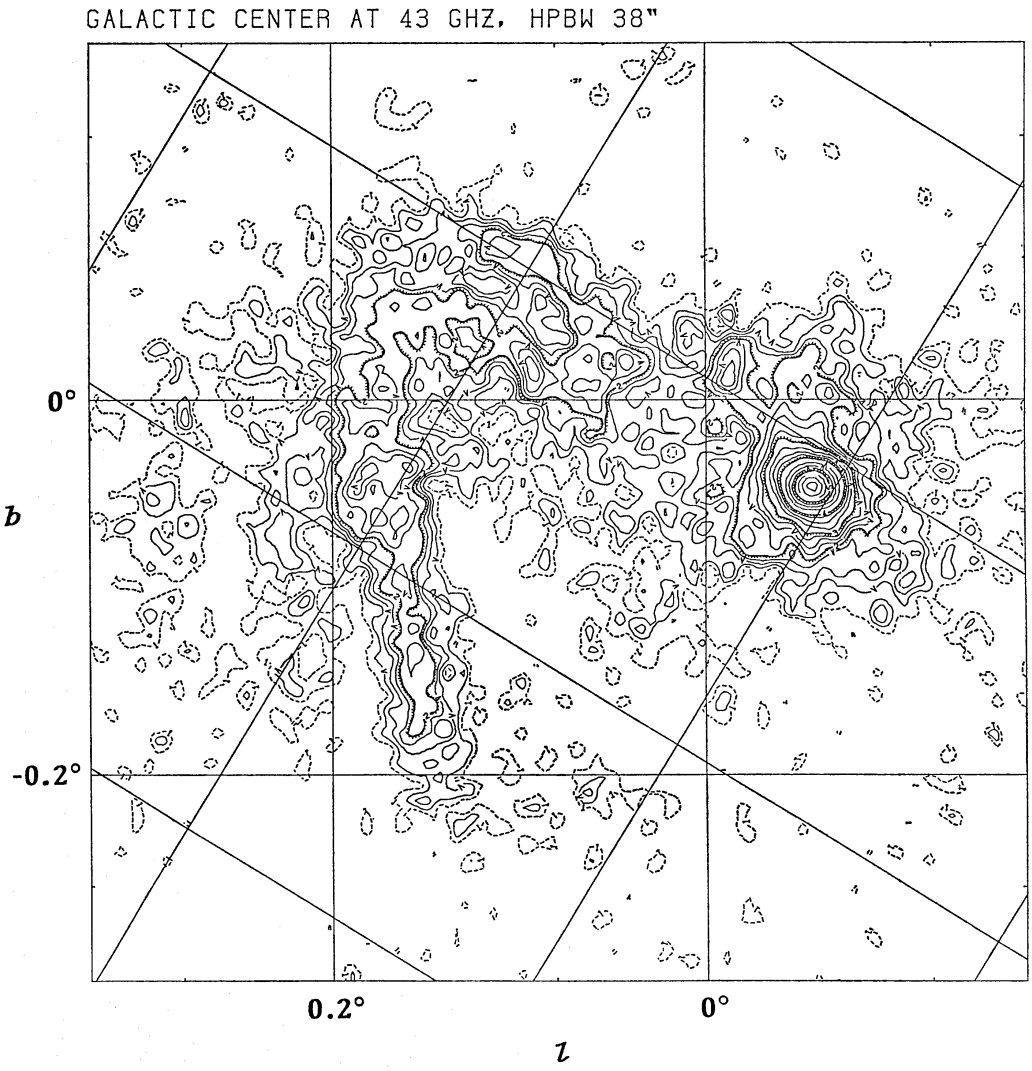

Fig. 1. 43.25-GHz continuum map of the galactic center taken with the 45-m telescope with a resolution of HPBW 38″. The hatched contours with numbers 1 through 6 correspond respectively to 1, 5, 10, 20, 50, and 100% of the peak flux density of Sgr A West, 11.6 Jy/38″-beam (=5.2-K $T_b=2.9\times10^{-18}$ W m^{-2} sr^{-1} Hz^{-1}).

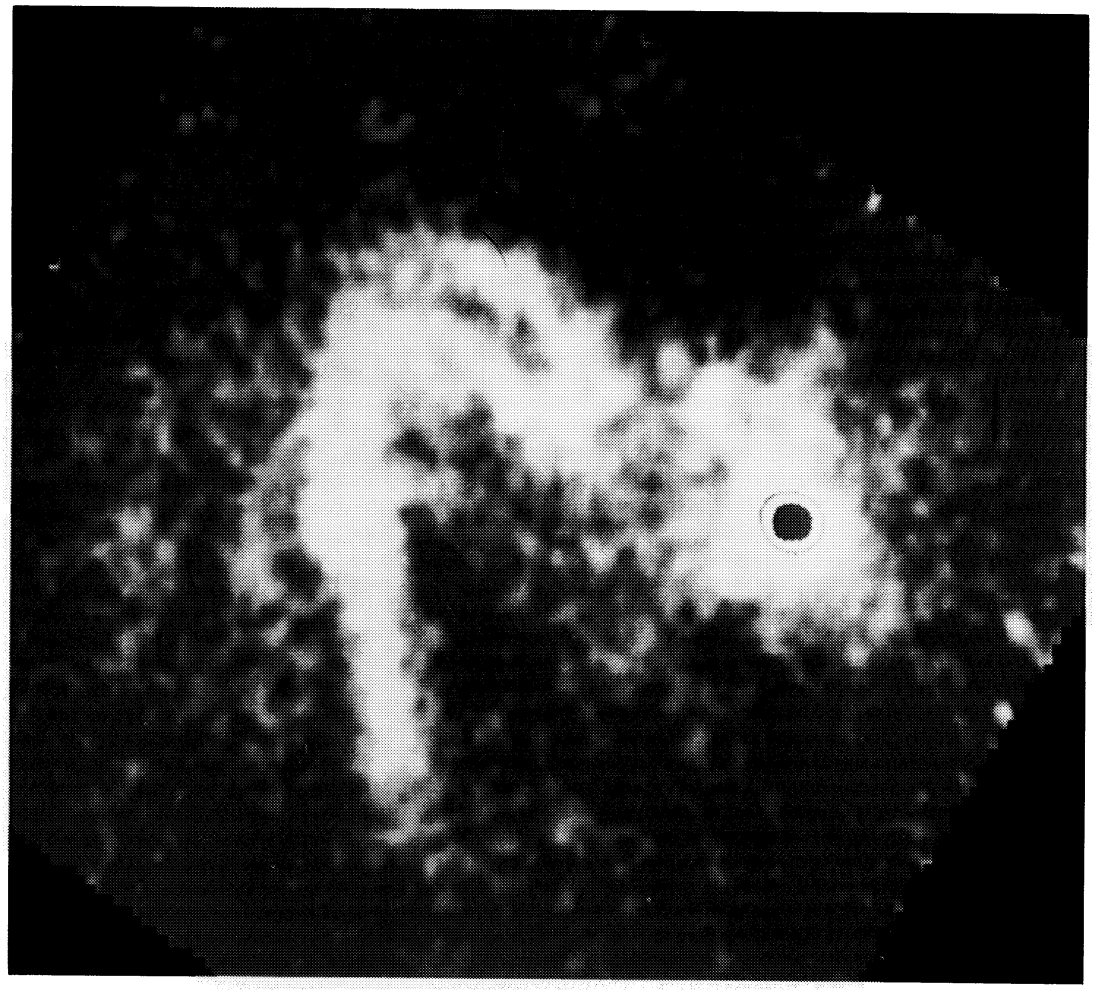

Fig. 2. The same as figure 1 but smoothed to a HPBW of 45″ and in a gray-scale representation.

both He-cooled at the 20-K stage. The center frequency and bandwidth were 43.25 and 0.5 GHz, respectively. The system temperature was about 500 K at the zenith. We detected one linear polarization with the feed system fixed to the telescope. The position angle of the polarization was fixed to the telescope on one night and was fixed to a position rotated by 90° from the first position on the other night. The observations on the two nights were added to give the total intensity. The observations were made in the beam-switching mode in which the main beam was switched at a frequency of about 500 Hz with a reference beam at a separation of 8° from the telescope axis. The main beam HPBW was 38″.5 and the reference beam had a HPBW of roughly 5°.

The mapping was made by scanning in the right ascension and declination directions alternately. The mapped region was $0^{\circ}.6 \times 0^{\circ}.6$ square in the equatorial coordinates centered at R.A.(1950)$=17^{h}43^{m}00^{s}$ and Decl.(1950)$=-28^{\circ}52'00''$. The scan interval was 15″ and the sampling of data was done also at every 15″ along each scan. One scan took 30 s and therefore one map took 1.2 hr to make. We mapped the region four times on one night and repeated the same on the other night with a feed rotated by 90°. The effective integration time per beam area was 12 s on the

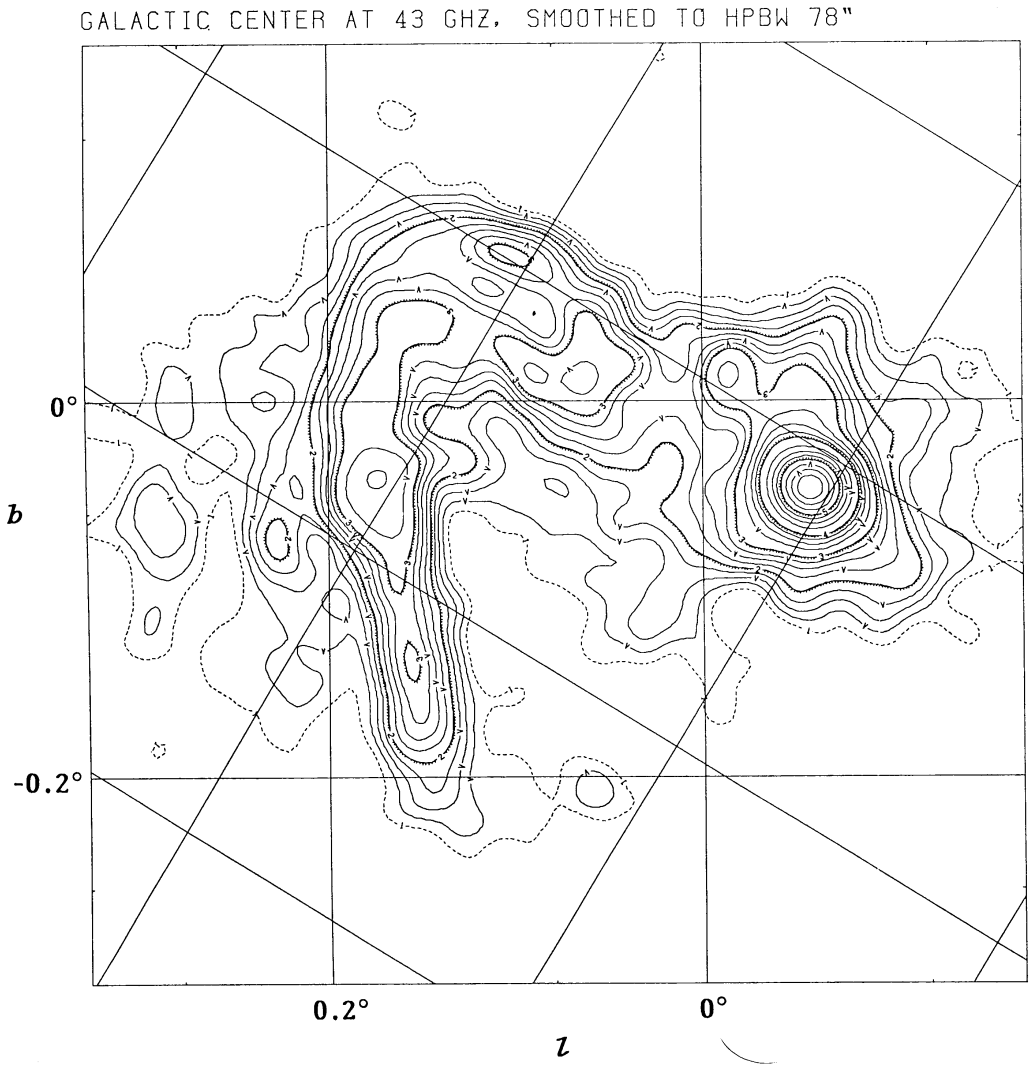

Fig. 3. The same as figure 1 but smoothed to a HPBW of 1′.3, the same resolution as the 10.7-GHz map of Pauls et al. (1976). The peak flux density of Sgr A is 24 Jy/1′.3-beam (=2.6-K $T_b=1.5\times10^{-18}$ W m^{-2} sr^{-1} Hz^{-1}).

final map which is the superposition of the eight maps. This gives a calculated rms noise on the map of 10-mK T_a. The rms noise on the resultant map is estimated as about 30-mK T_b, or roughly 10-mK T_a, consistent with the calculated rms.

The flux calibration was made referring to maps obtained for NGC 7027 prior to and after the observations. The flux density of NGC 7027 at 43.25 GHz was taken as 6.0 ± 0.3 Jy by extrapolating the spectrum determined by Harris and Scott (1976). The peak flux density of Sgr A was determined as 11.6 ± 1.2 Jy/beam area (HPBW=38″)$=5.2\pm0.5$-K $T_b=(2.9\pm0.3)\times10^{-18}$ W sr^{-1} m^{-2} Hz^{-1} and was assumed to be unpolarized. The intensity at any point on the map was normalized with the peak flux density of Sgr A and pointing was checked also using the Sgr A peak position. The data reduction was made by use of the astronomical reduction system, CONDUCT, at NRO. The scanning effects on each map were removed before superposition by applying the pressing method of Sofue and Reich (1979).

The beam shape was measured by mapping 3C 273. The beam was almost circular at half maximum. The major side lobes were found to be below −20 dB of the beam center in power. This means that the side-lobe contribution from Sgr A may appear below about 50-mK T_b level, only slightly higher than the rms noise (about 30-mK T_b), and below the lowest contours in figure 1.

The 43-GHz results are shown in figures 1 to 3. Figure 1 shows a contour map of Sgr A and the radio arc at the original resolution of HPBW 38″. Figure 2 is the same in a gray-scale representation, but smoothed to a Gaussian beam of HPBW 45″. Figure 3 shows the same but smoothed to a 1′.3 Gaussian beam in the contour diagram for comparison with the 10.7-GHz observations using the 100-m telescope (Pauls et al. 1976; Seiradakis et al. 1985).

3. Results

(i) Sgr A and the Halo

The Sgr A core is not resolved. However, from the apparent half-maximum diameter 64″ on the map, we can estimate the effective diameter of the core source as 51″ [$=(64''^2-38''^2)^{1/2}$]. The core is mainly contributed from the thermal source Sgr A West. The halo with fuzzy structures is resolved into some spurs and arcs within a distance of 6′ from Sgr A West. The nonthermal source, Sgr A East (e.g., Ekers et al. 1983), is hardly seen at 43 GHz.

Two spiral spurs run in the opposite directions away from the core, or Sgr A West: the northern (N) spur extends toward the positive latitude to G−0.03−0.01 ($l=0^\circ.03$, $b=-0^\circ.01$), where it encounters a ridge running from G−0.03+0.005 through G−0.08−0.015 (see figure 4). The N spur seems to bifurcate into two arms composing a lobelike structure. The southern (S) spur extends toward the south to G−0.09−0.10 composing a loop centered on G−0.07−0.10. Both the S and N spurs appear to compose a two-armed spiral feature or a two-lobed structure emerging from Sgr A West. These spurs are well recognized on an 18-cm VLA map (H. S. Liszt, private communication). A part of the S spur is also recognized on the 6-cm VLA map by Ho et al. (1985), which they call the "wisp." Another long spur extends toward the east from G−0.01−0.09 almost reaching the southern end of the radio arc.

(ii) Bridge

The Sgr A halo and the northern end of the radio arc is connected by the bridge which consists of a few complex filaments. One strong filament runs from G0.04+0.01 through G0.15+0.08, and another strong one runs from G0.06−0.03 through G0.15 +0.05. Radio recombination lines are detected along these two filaments (Pauls et al. 1976), which indicates their thermal origin. One more filament runs from G0.00−0.05 through G0.16−0.05 which merges with and coils around the arc at G0.18+0.05 to form a bright knot. The bridge starts from G0.03+0.00 toward the north. A gap is found between the bright part of the bridge and Sgr A West. The gap is located centered on G0.01−0.15 with a diameter of about $0^\circ.05$.

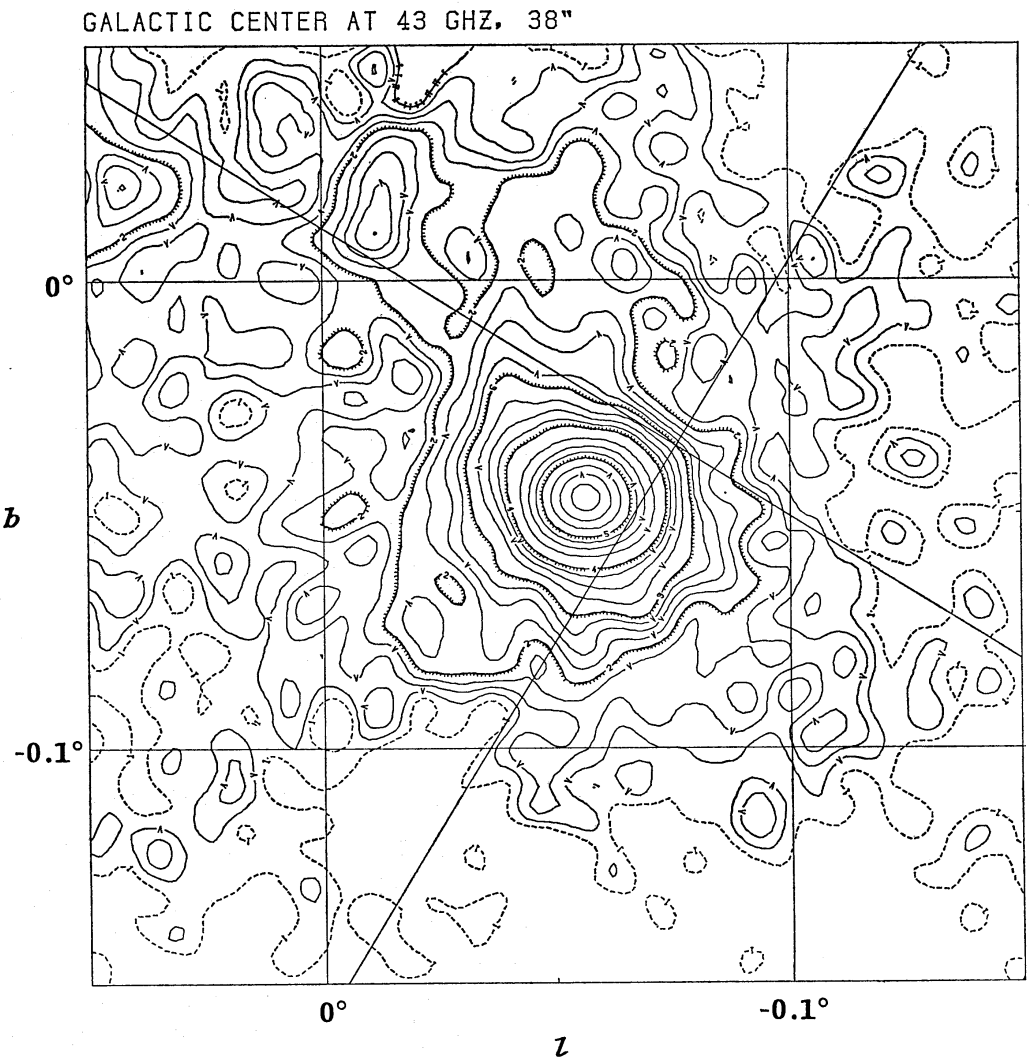

Fig. 4. Enlargement of figure 1 for the Sgr A core and halo. The contour unit is the same as in figure 1.

(iii) Radio Arc

The radio arc runs almost in a straight line perpendicular to the galactic plane. The arc is resolved into two areas: the main arc (G0.17 arc) runs from G0.16−0.20 through G0.18+0.01. Another arc (G0.19 arc) runs from G0.19−0.08 through G0.19+0.00. The former is brighter than the latter at 43 GHz, while the two are comparably bright on the VLA 18-cm map (H. S. Liszt, private communication): the VLA filament running from G0.195−0.05 through G0.19+0.07, which is one of the two most prominent filaments along the arc, is hardly seen on the 43-GHz map. This fact suggests that the spectrum of G0.19 arc is steeper compared to G0.17 arc.

Two other fainter arcs are found to the east of the radio arc. One (G0.23 arc) runs from G0.21−0.01 toward G0.22−0.12, and crosses the radio arc at G0.27−0.15. The other (G0.30 arc) is a faint arc running from G0.23+0.20 through G0.28−0.13, which might be an extension of the bridge.

Table 1. Flux densities of Sgr A at 43.25 GHz.*

Peak flux density/38″-Gaussian beam	11.6 Jy
Peak flux density/1′.3-Gaussian beam	24 Jy
Total flux assuming source diameter of 51″	32 Jy
Integrated flux within 1′.5-radius circle	40 Jy
Integrated flux within 6′-radius circle (core+halo)	82 Jy

* The errors are typically ±10%.

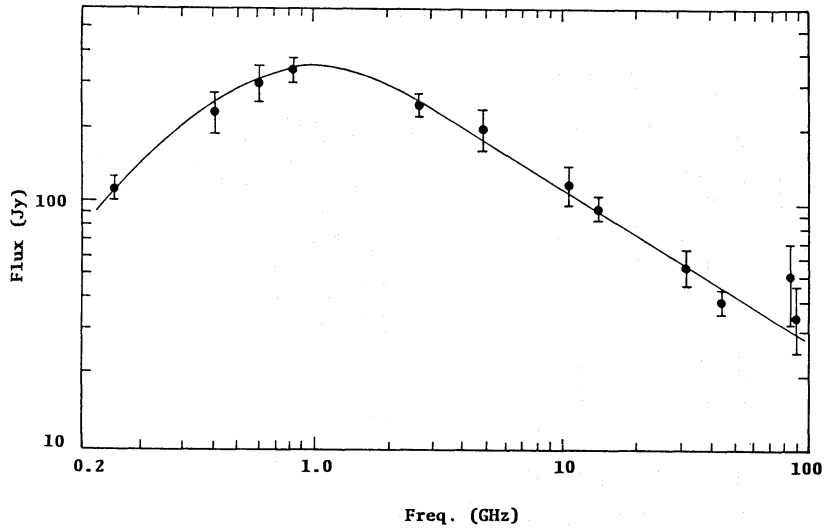

Fig. 5. Spectrum of Sgr A. The sources of data are: 160 MHz: Dulk and Slee (1974); 408 MHz: Little (1974); 610 MHz: Downes et al. (1978); 843 MHz: Mills and Drinkwater (1984); 2.7 GHz: Reich et al. (1984); 4.9 GHz: Downes et al. (1978); 10.7 GHz: Pauls et al. (1976); 15.5 GHz: Kapitzky and Dent (1974); 31.4 GHz: Downes et al. (1970); 43.25 GHz: this work; 85 GHz: Downes et al. (1970); 90 GHz: Dworetsky et al. (1969).

(iv) Flux Densities and Spectra

The total flux density of the Sgr A core assuming the source diameter of 51″ is estimated as 32±4 Jy. The integrated flux within a circle of radius 1′.5, where most of the strongest features are involved, is 40±4 Jy. The apparent flux density of Sgr A core+halo integrated within a circle of 6′ radius centered on Sgr A West [after the definition of Mills and Drinkwater (1984)] is 115±12 Jy. However, if we subtract the background emission by setting the mean brightness along the 6′ radius circle as the zero level, we obtain 82±10 Jy as the integrated flux within 6′ radius. Table 1 summarizes the estimated fluxes at 43.25 GHz of Sgr A.

The flux densities of Sgr A have been obtained at various frequencies (e.g., Mills and Drinkwater 1984). Figure 5 is a radio spectrum of Sgr A based on integrated fluxes obtained by observations with resolutions higher than 3′. The sources of the data are given in the caption to the figure. The spectrum has a turnover at around 1 GHz as is noted by Mills and Drinkwater (1984). The spectrum at higher frequencies up to 50 GHz is fitted with a power law of $\alpha=-0.62\pm0.05$, which indicates the non-thermal origin of the emission. This must be compared with the flatter spectral

Table 2. Peak flux densities S_p and spectral indices between 10.7 and 43.25 GHz* for discrete extended sources.

Position	S_p (Jy/1'.3-beam)		Spectral index	Remarks
	10.7 GHz	43 GHz		
G−0.05−0.05† 31		24	−0.18	Sgr A West
G−0.01+0.02† 3.7		3.0	−0.15	Halo
G 0.03−0.06 ..... 1.5		1.2	−0.2	Halo
G0.02−0.12 ..... 1.6		0.8	−0.5	Halo
G0.07+0.01† 2.7		3.0	0.08	Bridge
G0.07+0.04† 2.9		2.6	−0.08	Bridge
G0.09+0.01† 3.0		3.0	0.00	Bridge
G0.10−0.06 ..... 1.1		0.6	−0.4	Bridge
G0.10+0.08† 2.7		2.5	−0.06	Bridge
G0.15+0.04 ..... 2.2		2.4	0.06	Bridge
G0.16−0.15† 3.2		2.5	−0.17	Arc
G0.17−0.12 ..... 2.6		2.2	−0.12	Arc
G0.18−0.04† 4.6		3.6	−0.18	Arc
G0.18+0.00 ..... 2.8		2.7	−0.03	Arc
G0.24−0.08 ..... 1.2		1.2	0.0	Faint arc
G0.29−0.07 ..... 1.1		0.8	−0.2	Faint arc

* S_p at 10.7 GHz were taken from the map of Pauls et al. (1976) and those at 43.25 GHz were taken from figure 3, both of which have the same angular resolution of 1'.3 HPBW. The errors for the fluxes are typically ±10%, and the errors for the spectral index is typically ±0.1.

† Discrete sources listed by Pauls et al. (1976).

index of the peak fluxes between 10 and 43 GHz (−0.2) (see below). The steeper spectrum of the integrated flux is therefore due more to the nonthermal extended component surrounding Sgr A. In fact the spectrum above 50 GHz till 90 GHz seems to be flatter, where most of the emission comes from Sgr A West, although this is not conclusive because of the large errors at 80–90 GHz.

To see the nature of the radio emission of the features we determine spectral indices of the peak flux densities for several discrete sources listed by Pauls et al. (1976) and for some typical positions (table 2). We use the 10.7-GHz map of Pauls et al. (1976) and the smoothed 43.25-GHz map (figure 3), both in the same angular resolution of HPBW=1'.3. Peak fluxes were read from the maps and compared in the same unit of Jy/1'.3-beam to calculate the spectral index. Table 2 lists the positions, the fluxes, and calculated spectral indices between 10.7 and 43.25 GHz. The spectra for most of the positions are as flat as $\alpha=0$ to −0.2, except for a few weak sources like G0.02−0.12 which has a nonthermal spectrum. This result is consistent with the flat spectra obtained from three peaks in the arc (G0.16−0.15, G0.18−0.04, and G0.10+0.18) by Mills and Drinkwater (1984) and the flat spectra between 2.7 and 10.5 GHz derived for the extended sources in the galactic center region by Sofue (1985).

The flat spectra for sources along the bridge may be due to their thermal origin as has been proved from the recombination-line observations (Pauls et al. 1976). Sgr A West (core) is also thermal (Downes et al. 1978), which dominates the flux at higher frequencies. On the other hand, the radio arc is believed to be nonthermal from the peculiar morphology related to a strong magnetic field (Yusef-Zadeh et al. 1984).

This was confirmed by the detection of linear polarization (Inoue et al. 1984; Tsuboi et al. 1985; Seiradakis et al. 1985; Yusef-Zadeh et al. 1986). If the emission is due to synchrotron radiation, the lifetime of cosmic-ray electrons emitting at 43 GHz in a magnetic field of a few 10^{-5} G (Tsuboi et al. 1985) is as short as $\sim 10^6$ yr. Hence, the flat spectra obtained for the radio arc pose a severe problem of how such young energetic particles are accelerated or supplied in this region.

References

Altenhoff, W. J., Downes, D., Pauls, T., and Schraml, J. 1979, *Astron. Astrophys. Suppl.*, **35**, 23.

Brown, R. L., and Liszt, H. S. 1984, *Ann. Rev. Astron. Astrophys.*, **22**, 223.

Downes, D., Goss, W. M., Schwarz, U. J., and Wouterloot, J. G. A. 1978, *Astron. Astrophys. Suppl.*, **35**, 1.

Downes, D., Maxwell, A., and Rinehart, R. 1970, *Astrophys. J. Letters*, **161**, L123.

Dulk, G. A., and Slee, O. B. 1974, *Nature*, **248**, 33.

Dworetsky, M. M., Epstein, E. E., Fogarty, W. G., and Montgomery, J. W. 1969, *Astrophys. J. Letters*, **158**, L183.

Ekers, R. D., van Gorkom, J. H., Schwarz, U. J., and Goss, W. M. 1983, *Astron. Astrophys.*, **122**, 143,

Harris, S., and Scott, P. F. 1976, *Monthly Notices Roy. Astron. Soc.*, **175** 371.

Ho, P. T. P., Jackson, J. M., Barrett, A. H., and Armstrong, J. T. 1985, *Astrophys. J.*, **288**, 575.

Inoue, M., Takahashi, T., Tabara, H., Kato, T., and Tsuboi, M. 1984, *Pbul. Astron. Soc. Japan*, **36**, 633.

Kapitzky, J. E., and Dent, W. A. 1974, *Astrophys. J.*, **188**, 27.

LaRosa, T. N., and Kassim, N. E. 1985, *Astrophys. J. Letters*, **299**, L13.

Little, A. G. 1974, in *Galactic Radio Astronomy, IAU Symp. No. 60*, ed. J. F. Kerr and S. C. Simonson III (Reidel, Dordrecht), p. 491.

Mills, B. Y., and Drinkwater, M. J. 1984, *J. Astrophys. Astron.*, **5**, 43.

Oort, J. H. 1977, *Ann. Rev. Astron. Astrophys.*, **15**, 295.

Oort, J. H. 1985, in *The Milky Way Galaxy, IAU Symp. No. 106*, ed. H. van Woerden, R. J. Allen, and W. B. Burton (Reidel, Dordrecht), p. 349.

Pauls, T., Downes, D., Mezger, P. G., and Churchwell, E., 1976, *Astron. Astrophys.*, **46**, 407.

Reich, W., Fürst, E., Steffen, P., Reif, K., and Haslam, C. G. T. 1984, *Astron. Astrophys. Suppl.*, **58**, 197.

Seiradakis, J. H., Lasenby, A. N., Yusef-Zadeh, F., Wielebinski, R., and Klein, U. 1985, *Nature*, **317**, 697.

Sofue, Y. 1985, *Publ. Astron. Soc. Japan*, **37**, 697.

Sofue, Y., and Handa, T. 1984, *Nature*, **310**, 568.

Sofue, Y., and Reich, W. 1979, *Astron. Astrophys. Suppl.*, **38**, 251.

Tsuboi, M., Inoue, M., Handa, T., Tabara, H., and Kato, T. 1985, *Pbul. Astron. Soc. Japan.*, **37**, 359.

Yusef-Zadeh, F., Morris, M., and Chance, D. 1984, *Nature*, **310**, 557.

Yusef-Zadeh, F., Morris, M., Slee, O. B., and Nelson, G. J. 1986, *Astrophys. J. Letters*, **300**, L47.